Assessing health and environmental impacts of solvents for producing perovskite solar cells

Rosario Vidal,[a,*] Jaume-Adrià Alberola-Borràs,[a,b] Severin N. Habisreutinger,[c] Joaquín-Luis Gimeno-Molina,[a] David T. Moore,[c] Tracy H. Schloemer,[c, d] Iván Mora-Seró,[b] Joseph J. Berry,[c] and Joseph M. Luther[c, *]

[a] Department of Mechanical Engineering and Construction, GID, Universitat Jaume I, Av. SosBaynat s/n, 12071 Castelló, Spain

[b] Institute of Advanced Materials (INAM), Universitat Jaume I, Av. Sos Baynat, s/n, 12071 Castelló, Spain

[c] National Renewable Energy Laboratory, Golden, Colorado 80401, United States

[d] Colorado School of Mines, Golden, Colorado 80401, United States

*Corresponding author. E-mail: vidal@uji.es, joey.luther@nrel.gov

Abstract

Halide perovskites are poised as a game-changing new semiconductor system with diverse applications in optoelectronics. Industrial entities aim to commercialize perovskite technologies because of high performance, but also because this type of semiconductor can be processed from solution, a feature enabling low cost and fast production. Here we analyze the health and environmental impacts of eight solvents commonly used in perovskite processing. We consider first and higher order ramifications of each solvent on an industrial scale such as the solvent production, use/removal, emissions and potential end-of-life treatments. Further, we consider the energy of evaporation for each solvent, air emission, condensation and subsequent incineration, reuse or distillation for solvent recycling and apply a full end-of-life analysis. For human health impact, we use the 'USEtox' method, but also consider toxicity data beyond carcinogenic classifications. We find that dimethylsulfoxide (DMSO) has the lowest total impact being the most environmentally friendly and least deleterious to human health of the solvents considered. The analysis of these solvents on human health and the environment provides guidance for sustainable development of this new technology.

Introduction

In 2009, an unassuming finding was reported[1] that nanocrystals of methylammonium lead triiodide deposited on titanium dioxide produced a photovoltaic (PV) device with sunlight to electricity conversion at a modest 3.8% efficiency. This seminal work and subsequent reports[2,3] have inspired a renaissance in hybrid organic/inorganic crystalline material research, with halide perovskite semiconductors (simply referred to here as perovskites) as one of the hottest topics in science. The PV efficiency now exceeds 25% for a single junction and over 29% as a multijunction technology paired with Si[4]. Solution-processed perovskites are poised for wide commercialization not just in PVs but in products like displays, solid state lighting, optical/radiation detection, *etc*[5,6].

PVs are a large volume application for perovskites, with important implications on sustainability because, if existing hurdles to commercialization are overcome, perovskite PVs could be produced rapidly, with high efficiency at low cost to provide massive amounts of sustainable electricity[7]. Solution-based perovskite production makes it inherently different than previous semiconductors and therefore careful consideration of this aspect of manufacturing is warranted. Typically, polar aprotic solvents are used to dissolve precursor salts which when mixed, cast and annealed, form the polycrystalline perovskite film. The solvent chemistry is manipulated to yield good device performance, but for large-scale production, the environmental and human health aspects of processing must also be evaluated. While a full life cycle analysis (LCA) has yet to be published, it seems likely that, aside from the unique deposition of perovskites, the remainder of industrial manufacturing would be analogous to that of existing/established thin film PV technologies.

While the fact that PV perovskites contain Pb spurs many discussions, solvent use at the industrial scale has not been analyzed in depth (See Supplementary Note 1 for health and environmental concerns in other industries). Some polar aprotic solvents used for perovskite film fabrication may cause concern due to their toxicity[8–11]. The most commonly used solvent for perovskite layer deposition, N,N-dimethylformamide (DMF) is included in the Candidate List of Substances of Very High Concern (SVHC), as part of the Regulation by the European Chemical Agency (Registration, Evaluation, Authorization and Restriction of Chemicals, REACH). The authorization process "*aims to ensure that SVHCs are progressively replaced by less dangerous substances or technologies where technically and economically feasible alternatives are available*".[12] Moreover, DMF, and comparable solvents such as N,N-dimethylacetamide (DMAC), and N-Methyl-2-pyrrolidone (NMP) are recognized as toxic to the human reproductive systems. Other similar solvents such as gamma-butyrolactone (GBL); 1,3-dimethyl-3,4,5,6-tetrahydropyrimidin-2(1H)-one (DMPU) and tetrahydrofuran (THF) are labeled "dangerous". For mass production of perovskites, appropriate handling of solvents must be considered during the initial development phase to mitigate environmental impacts while optimizing performance.

Material and energy flows and emissions can be quantified across a solvent's value chain[13]. While the impacts of solvent production are included in a few perovskite LCAs (DMF[14–19], mixtures of DMF and DMSO[20,21] (dimethyl sulfoxide) and GBL[21,22]) in-depth environmental impact (from cradle to grave analysis) of perovskite deposition is lacking. For more in-depth descriptions of reported perovskite solvents, see **Error! Reference source not found.**. Solvent mixtures or solvents with additives offer additional control during deposition and some can be described as "green solvents". For example, mixtures of DMSO, GBL and DMF such as: GBL+alcohol+acid[23], DMSO+2-butoxyethanol[24], DMSO+2-methylpyrazine[25], and DMF:DMSO+pyridine[26] have been used; but also other possible formulations such as PolarClean (Methyl 5-dimethylamino-2-methyl-5-oxopentanoate)[27], methylamine+acetonitrile[28] and 1,3-dimethylimidazolidin-2-one (DMI)[29] have been reported. The aim of those studies was to demonstrate viable alternatives for DMF, which are conceivably less-hazardous, non-toxic and have a smaller environmental footprint. A quantitative critical assessment of these replacement solvent systems is still needed prior to large scale-industrial use.

Currently, the best available model for characterizing HHT of chemicals is USEtox[30]. However, many characterization factors are insufficient based on the latest data. Following the original USEtox substance

72   databases[31], new chemical regulations have been enforced through REACH regulations. These require chemical
73   risk assessments for humans and the environment before chemicals are placed on the market. Consequently,
74   additional physicochemical property data and new toxicological endpoints are now available for thousands of
75   chemical substances[32].

76   Here we study the HHT and other environmental impacts included for human health of eight polar aprotic
77   solvents used for perovskite deposition: DMF, DMSO, DMAC, NMP, DMI, GBL, THF and DMPU. Both, single-
78   solvent and co-solvent analyses are presented. The impacts of solvent production, removal and emissions are
79   considered. A comprehensive environmental comparison of solvents for perovskite layer deposition demands an
80   LCA methodology. Fate and exposure models are then applied to determine missing human health
81   characterization factors for several solvents and to update existing values with available toxicity data published
82   from the registration dossiers submitted to the European Chemical Agency (ECHA) under the REACH
83   regulation[12]. USEtox[31] is modified with newly available toxicity data for detrimental impacts on human health
84   beyond the binary "carcinogenic" classification. Then, post-processing solvent removal is modelled for different
85   scenarios. Heat or air flow require additional energy and are calculated. Some solvents do not have life-cycle
86   inventories for their production; however, as we show, it can be estimated from published literature. We model
87   the following potential scenarios: direct emission of solvent vapor to urban air, solvent condensation with
88   subsequent incineration, and solvent recovery (with and without further purification).

Results

90   For each solvent, we consider the environmental impacts arising from industrial production, use, end-of-life
91   (EOL) costs, safety, and health hazard characteristics[33]. Figure 1 shows the LCA of perovskite PV manufacturing
92   using solvents. Solvent transport to the perovskite factory, the removal from the thin film during drying, solvent
93   emission, treatment for energy recovery and solvent recovery are illustrated. Four scenarios are considered for
94   solvent EOL. In scenario 1, solvents are emitted directly to the environment, common at lab and pre-industrial
95   scale. In scenario 2, the solvents are condensed and incinerated (with energy recovery), with only a small
96   fraction being directly emitted. Incineration without energy recovery is also included in the Supplementary Note
97   8. In scenario 3, the condensed solvent (with high purity) is assumed to be reused. Scenario 4 is similar to 3
98   except the condensed solvent is distilled and the fraction not distilled is incinerated (with energy recovery). All
99   scenarios share the solvent production and the solvent removal steps. The modeling for solvent production,
100   removal, condensation, incineration and distillation are detailed in the Methods section.

101   Scalable production of perovskites benefits from low capital and operational expenditure including energy
102   consumption, materials costs, post-treating of production waste and toxic side products[11]. For solvent choice,
103   additional costs beyond acquisition should be considered, namely the energetic cost of removal and treatment
104   as well as possible reagents for the treatment at EOL. Further, it is important to quantify the amount of solvent
105   needed. In scalable deposition processes such as blade coating, the amount of solvent, calculated using in-house
106   expertise, is 2.5 mL·m^{-2} for the deposition of a perovskite layer of 500 nm. One expects similar ink transfer
107   efficiencies with spray coating and roll-to-roll processes. This equates to 3500 liters of solvent needed for a 1
108   GW factory assuming module efficiencies of 15% and a high module yield[5].

Solvents selection and toxicological classification

110   Obviously, there are strict requirements for a solvent to properly coordinate ions of perovskites. Hamill et al.[34]
111   demonstrated Gutmann's donor number[35] (DN) as a parameter for the coordinating ability of a solvent with
112   Pb^{2+}. Low DN solvents interact weakly with Pb^{2+}, instead favoring complexation between Pb^{2+} and iodide. High
113   DN solvents coordinate more strongly with the Pb^{2+} center, which in turn inhibits iodide coordination and stalls

114 perovskite crystallization. Varying the concentration of high-DN additives in precursor solutions tunes the
115 strength of Pb–solvent interactions, allowing finer control over crystallization and the resulting morphology of
116 perovskite active layers[11,36–38].

117 Aprotic solvents with DN between 18 and 33 defined by Hamill[34] included in Table 1 are the subject of this
118 assessment. DMF, DMSO, GBL, NMP, DMAC and DMPU are used extensively in literature (expressed by
119 "Common"). THF and DMI are used less frequently (see Table 1).

120 *Table 1. Solvents selected ordered by donor number. ECHA classification & labelling[12]. C= carcinogen; R= toxic to reproduction. The sub*
121 *index p means potential and the sub index r means recognized.*

Name	Acronym	CAS	Labeling & property of concern	DN[35]	References
-butyrolactone	GBL	96-48-0	Danger	18	Common
Tetrahydrofuran	THF	109-99-9	Danger, C_p	20	39–41
N,N-dimethylformamide	DMF	68-12-2	Candidate list SVHC, R_r	26.6	Common
N-methyl-2-pyrrolidone	NMP	872-50-4	Danger, R_r	27.3	Common
Dimethylacetamide	DMAC	127-19-5	Candidate list SVHC R_r	27.8	Common
1,3-dimethylimidazolidin-2-one	DMI	80-73-9	Danger	29	29,42,43
Dimethyl sulfoxide	DMSO	67-68-5	No hazards	29.8	Common
1,3-dimethyl-3,4,5,6-tetrahydropyrimidin-2(1H)-one	DMPU	7226-23-5	Danger R_p	33	Common

122 The European Chemical Agency classifies DMF and DMAC as SVHCs and toxic to reproduction**Error! Reference**
123 **source not found.** These include endocrine disruptors and substances that are carcinogenic, toxic to
124 reproduction or very persistent.

125 The remainder of solvents are labelled "danger", except DMSO which is not classified (although "not classified"
126 in the hazard statement does not mean nonhazardous, see Supplementary Note 1). NMP is classified as toxic to
127 reproductive systems and DMPU is potentially toxic. THF is potentially carcinogenic, however, in the
128 toxicological information from registered substances, it is concluded[12]: "*THF should not be rated for*
129 *carcinogenicity. However, there is a harmonized classification for this substance as a Category 2 carcinogen*
130 *under the EU CLP classification system (EC No 1272/2008)*". Supplementary Table 3 includes the hazard
131 statement for each solvent along with properties such as boiling point, vapor pressure and lower explosive limit
132 that influence potential environmental impacts.

133 Manufacturing, removal and EOL also have environmental effects for each solvent. For example, DMSO, the
134 least hazardous as indicated in Table 1, has a higher boiling temperature and lower vapor pressure than DMF
135 and THF, therefore, higher energy consumption is required for the removal of DMSO resulting in additional
136 environmental impacts. A critical assessment of the *total potential effects* will better guide solvent tradeoffs.

Human health toxicity

138 USEtox provides a good starting point to estimate HHT with regards to environmental impact, but as we show,
139 can be expanded and improved by breaking down the potential causes beyond the simple carcinogenic
140 classification. We use updated toxicity data, as explained in the Methods section *Determination of new human*
141 *health toxicity characterization factors.* For urban air emission, Table 2 recompiles the initial characterization
142 factors for HHT impact category with USEtox 2.11, measured as number of cases of any identified condition per
143 kg of solvent emitted. Toxicity data are in Supplementary Tables 4-11.

Emission to urban air	DMF	DMSO	DMAC	NMP	DMI	GBL	THF	DMPU
Initial USEtox carcinogens	0	0	0	9.64E-09	n/a	0	6.77E-08	n/a
Initial USEtox non-carcinogens	2.91E-06	n/a	0	n/a	n/a	0	n/a	n/a
Estimated carcinogens	0	0	0	0	0	0	0	0
Estimated non-carcinogens	2.61E-06	4.89E-08	4.61E-07	2.22E-07	5.91E-07	6.78E-07	7.60E-08	3.23E-06
Liver	1.70E-06		1.31E-07					
Spleen								1.49E-06
Benign neoplasm						2.96E-09		
Systemic toxicity		1.15E-08	1.34E-07	3.54E-08		6.41E-08	3.13E-08	
Chronic nephropathy				6.63E-09				
Digestive-Anemia		5.41E-10						
Upper respiratory irritation		2.97E-08		5.27E-08				
Maternal disorders, Infertility	4.53E-07			5.36E-09	2.95E-07			1.49E-06
Fetotoxicity (growth reduction)		7.22E-09			2.95E-07	6.11E-07	4.47E-08	2.49E-07
Fetotoxicity (skeletal variations)	4.53E-07		1.97E-07	1.22E-07				

While DMF is the only solvent considered by USEtox 2.11 to be carcinogenic, general toxicity and other sources of HHT-relevant data exist for all of the solvents studied. NMP and THF are arguably carcinogenic according to USEtox, however the measured carcinogen characterization factor as assessed with the new model is zero. The potential carcinogenic effects are discussed for DMF, GBL and THF in the REACH[12] registration dossiers and it is concluded that no carcinogenic risk exists for humans.

To assess the global impact of those solvents on human populations, such characterization metrics should be considered in addition to direct damage to human health, impacts on the environment such as climate change, ecosystem quality and resource scarcity, *etc.* Such a metric which encompasses direct effects via HHT and higher-order environmental effects impacting human health, is the disability-adjusted life year (DALY). DALYs are defined as a measure of disease burden composed of the sum of the years of life lost due to premature mortality in the population, and the years lost due to disability for people living with a health condition or its consequences.

We further modify USEtox by converting all data into DALYs for each of the causes identified, see Supplementary Table 13. USEtox gives the same weighting factor for all non-carcinogenic causes. However, the consequences for an upper respiratory irritation or a skeletal malformation of a fetus, for example, are significantly different. These weighting factors are applied to the characterization factors in Table 2 and the results are shown in **Error! Reference source not found.**a. DMF has the highest DALYs, followed by DMAC. Note DMF and DMAC are SVHC, Table 1. The main consequence is fetotoxicity; namely DMF, DMAC and NMP are recognized as toxic for reproduction. Other causes are almost negligible with the exception of impacting the liver for DMF and the spleen for DMPU.

Human health characterization factors extracted from USEtox 2.11 shown in **Error! Reference source not found.**b and Table 2 use the new toxicological data for additional estimated values. All solvents show increased characterization factors except for DMF and THF, though DMF remains the most damaging in this impact category. The modified method highlights the cases of fetotoxicity with respect to other non-carcinogenic causes.

Solvent removal

While solution processability of perovskites is touted as low cost, leveraging low capital expenditure production equipment compared to established semiconductor processing, solution-based fabrication requires additional disposal considerations. The most obvious consideration is the removal of solvent as the perovskite film dries. This step is critical for forming high performance solar cells. For high production rates, the solvent must be forced to dry quickly. We calculated the required drying energy using the substrate temperature and air velocity as inputs. This energy consumption adds to the LCA. We consider the heat for liquid to gas phase transitions and added air flow using either laminar or turbulent convective mass transfer, see Methods section.

Using convective mass transfer (Table 3 and Supplementary Tables 15 and 16), the temperatures selected achieve an evaporation time of less than 2 seconds for a surface with a characteristic length of 1 m and web width of 1 m for 500 nm film thickness. Note that in the turbulent drying scenario, no heating is required for DMF and DMAC, and only the kinetic energy of the air is included, which significantly reduces the total energy consumption. The scenario of turbulent convective mass transfer has the lowest values. However, turbulent flow is not sufficiently assessed[44]. The exact processing conditions would likely be between these values and will need further optimization taking into consideration the achievable module performance.

Table 3. Evaporation rate and energy required for drying time below 2 seconds per m^2. Two scenarios: a) laminar flow b) turbulent flow. Common considerations: thin film of 1x1 m^2 and thickness of 500 nm, 2.5 mL·m^{-2} of solvent, solvent concentration = 30% of lower explosive limit, room temperature of 25 ºC with 10ºC increments for temperature.

	Laminar convective mass transfer		Air velocity: 4 m/s	Turbulent convective mass transfer		Air velocity: 30 m/s
Solvent	Temp (ºC)	Evaporation rate(g/(s.m^2))	Energy (kJ/kg)	Temp (ºC)	Evaporation rate(g/(s.m^2))	Energy (kJ/kg)
DMF	90	1.51	5247.8	50	1.93	35.5
DMSO	120	1.71	6123.4	80	2.10	1633.1
DMAC	90	1.19	5389.0	50	1.28	36.4
NMP	120	1.28	9537.3	80	1.47	2543.8
DMI	150	1.61	11003.5	100	1.47	3969.0
GBL	140	1.73	12322.0	90	1.61	3774.3
THF	25	2.58	0.8	25	2.35	43.9
DMPU	170	1.43	9348.9	110	1.30	3523.8

THF is capable of evaporating at room temperature in both regimes. Kinetic energy is practically negligible at the air velocities considered. Temperature is the most significant factor in the energy requirements of each solvent, but vapor pressure, specific heat, density and lower explosive limit also contribute.

Life cycle assessment

The environmental impacts affecting human health during the life cycle of the solvents used in perovskite film manufacturing, including production, removal and EOL for the four scenarios considered are plotted in **Error! Reference source not found.**. In panel (a), the impacts are broken down by category. Three categories are highlighted: Toxicity, global warming and fine particulate matter. The remaining categories have been grouped as "others" (the impacts of human health from stratospheric ozone depletion, ionizing radiation and ozone formation, see Supplementary Table 17 for midpoint environmental impacts). The HHT for solvent emission is estimated with a new method, described in the *Human health toxicity* section. In panel (b), the impacts are broken down by life cycle phases.

202 Focusing on scenario 1, which does not include EOL treatment, DMF presents the highest impact during
203 emission (**Error! Reference source not found.**b), however, when the entire life cycle is considered, others
204 including NMP have much greater impact due to high energy consumption during production. Energy
205 consumption is directly related to the increased impact of global warming (Supplementary Figure 1) and the
206 impact of particulate matter. At the opposite end, DMSO has the lowest impact followed by DMPU and DMAC.

207 Incineration following condensation without energy recovery is more harmful to the environment than direct
208 emission into the atmosphere and should always be avoided (Supplementary Note 8). Adopting an EOL
209 treatment (scenarios 2-4) reduces the environmental impact and the HHT with two exceptions (see also
210 Supplementary Figure 2). The energy consumption by a condenser for THF is excessive, see **Error! Reference
211 source not found.**b, therefore other alternatives should be analyzed like using a membrane as a pre-
212 concentration step for THF recovery[45].

213 The second exception is the incineration of DMSO (**Error! Reference source not found.**b). The reagents needed
214 to neutralize sulfur increase toxicity to human health (**Error! Reference source not found.**a). Other alternatives
215 should be analyzed if DMSO recovery is not possible. Wastewater treatment containing DMSO is difficult
216 because aerobic biological processes cannot effectively decompose DMSO, and anaerobic biological processes
217 produce noxious compounds (dimethyl and hydrogen sulfides). However, DMSO is efficiently decomposed into
218 methanesulfonic acid using UV/H_2O_2 process or ozone based oxidation processes[46].

219 Controlled emissions are critical for DMF, DMAC and DMPU for significant reductions of HHT (**Error! Reference
220 source not found.**a and Supplementary Figure 2). Further analysis beyond hazard statement of Table 1 and
221 Supplementary Table 3, shows the impacts of DMSO, DMPU, DMAC and DMF are lower than that of DMI, GBL,
222 NMP and THF. Note, GBL and DMI are solvents with the highest impact, however some references[23,29] consider
223 them as non-hazardous potential alternatives to other solvents, which create less environmental impact.

224 Scenario 3 (direct solvent recovery using a condenser) is an ideal option but must be tested to determine if the
225 purity of the recovered solvent is sufficient. Some solvents are much more prone to deprotonation and
226 production of side complexes that would require a more complex purification process. If not adequate, scenario
227 4 would be more realistic. Regardless of whether distillation is required, solvent recovery (scenarios 3 and 4) is
228 more environmentally friendly than scenario 2 and should be explored by researchers. Other alternatives such
229 as direct distillation without condensing and less energy intensive separation routes should also be researched.
230 Note in **Error! Reference source not found.**b the solvent recovered is subtracted from the solvent production
231 and the energy recovered is expressed with negative values to indicate the beneficial effect.

Discussion

233 To put this study in context, we compare the solution-based perovskite production with deposition of other PV
234 absorbers, specifically amorphous silicon in heterojunction cells (SHJ) with an efficiency of 20% and CdTe with an
235 efficiency of 15% for a 1 GW scale plant (see the detailed assessment in the Supplementary Note 9). The
236 perovskite solvent chosen here is DMF, the most problematic of the solvents studied from an HHT perspective.
237 With no EOL, *i.e.* directly emitted to the atmosphere, the HHT and environmental impacts for perovskite
238 production are at least 30x lower, which are all small in comparison to analogous electronic technologies, *e.g.*
239 the production of 30,000 17" LCD displays[47]. Thus, in the case of DMSO, the results are even more favorable for
240 the environment. The total solvent quantity is marginal even at the industrial scale thus we conclude that a
241 significant impact on human health due to solvent use is not likely. However, future legislation could limit the
242 large-scale industrial use of DMF or other relevant solvents, which is why we encourage further development of
243 greener processes

244   This methodology, focusing on the utilization of solvent for the fabrication of PV devices, highlights the
245   comparatively lower human environmental impacts of DMSO in this context, which is in good agreement with
246   recommendations in other industries (see Supplementary Table 1); however DMSO does present some
247   challenges (see Supplementary Note 1). In addition, we demonstrate a general methodology for analyzing the
248   impact of a combination of solvents which can inform new solvent strategies aimed at reducing their
249   environmental impact; a vital step towards industrializing perovskite PVs.

250   This work should be considered a roadmap for researchers to further develop less hazardous solvents. The
251   rationale for using solvent combinations is to finely tune the interactions between the solvate and to optimize
252   the nucleation and crystallization dynamics. Recently, strategies to tune these dynamics have been proposed,
253   for example, mixing PbS nanocrystals into the solution in DMSO.[48] This strategy provides vital insights into how
254   additives can improve DMSO for high-performance devices and informs potential new approaches to
255   manufacturing using DMSO as the main solvent (also see Supplementary Table 23). Also noteworthy are the
256   promising results of DMSO/2-butoxyethanol[24] and acetonitrile/methylamine[49] in roll-to-roll processes (see
257   Supplementary Table 24).

258   Analysis of solvent mixtures is considered here for DMF / DMSO combinations (See Supplementary Note 11).
259   Additional inputs include density, excess molar enthalpy and excess molar heat capacity of the mixture. Higher
260   DMSO concentration (Supplementary Figure 4) and adopting an EOL treatment (scenarios 2-4) reduces the
261   human health and environmental impacts, except for incineration when DMSO volume fraction exceeds 0.5.

262   In summary, we have assessed the human health and environmental impacts for the manufacturing, removal
263   and EOL of solvents for perovskite deposition. USEtox, the best current characterization model, is modified by
264   breaking down the potential health impacts beyond the generic carcinogen classification, updated with the
265   latest available toxicity data. We convert the relevant metrics to DALYs and find that DMF is the most
266   consequential, followed by DMAC. While more work remains to further improve the HHT characterization
267   factors with the modified method presented here, we find that DMSO has the lowest human health and
268   environmental impacts in each of the scenarios analyzed: direct emission, incineration with energy recovery,
269   solvent recovery without and with distillation. For all solvents considered, solvent recovery is more
270   environmentally friendly than incineration even with energy recovery regardless of whether distillation is
271   required. We conclude that work targeting the transition to industrial scale production should consider the
272   impact of solvents which might affect human health and the environment. Our analysis suggests DMSO as the
273   main solvent offers the lowest negative footprint on an industrial scale but any viable solvent must still enable
274   critical performance metrics such as power conversion efficiency and module stability. This analysis provides
275   guidance for solvent choice for perovskite PV and an approach to compare the human health and environmental
276   impacts of other nascent and established "green" energy technologies.

METHODS

Human health environmental impacts

The environmental impact categories considered here and included in the human health area of protection are toxicity from USEtox[31,50,51] or from the improved methodology developed in this paper. The common unit for reporting and comparison of these categories is DALYs. Other impact categories: global warming, toxicity, stratospheric ozone depletion, ionizing radiation, ozone formation and fine particulate matter formation, are obtained from ReCiPE 2016 v1.1 with the Endpoint method and the Hierarchist version[52]. Environmental impacts, calculated with ReCiPE Midpoint method, are also included. At the midpoint level, impact categories are not grouped in areas of protection.

Determination of new human health toxicity characterization factors

From OECD QSAR Toolbox 4.3[53], data is extracted that incorporates various modules and databases of the EPI Suite™ developed by US EPA[54] to assist in the risk assessment of chemicals[55], and introduced in USEtox for human exposure and toxicity model[31] which was implemented in Microsoft® Excel®[51]. The following characteristics were implemented: molecular weight, dissociation constant for organic acids or bases, octanol-water partitioning coefficient, organic carbon-water partitioning coefficient, Henry constant, vapor pressure, water solubility, degradation rates in air, water, soil and sediment, and bioaccumulation factors for fish.

Toxicity data is extracted from published data of the registration dossiers submitted to European Chemical Agency (ECHA) under REACH Regulation[12]. Previously, REACH was used as a potential data source for ecotoxicity[32,56–59].

Registers of toxicity data include: the route (oral or inhalation), the test animal (humans, rats, mouse, rabbits, etc.), dose exposure time (chronic for more than 210 days, subacute for 2-4 weeks and subchronic), descriptor (The No-Observed-Adverse-Effect Level, NOAEL/NOAEC or the Lowest-Observed-Adverse-Effect Level, LOAEL/LOAEC), the value of the descriptor with the appropriate corrections if the exposure is different than 24 h· day^{-1} and 7 days·week^{-1} (the units are mg·kg^{-1} bodyweight·day^{-1} for oral ingestion and mg·m^{-3} for inhalation), disease or organ affected and descriptions of the observed effects. Toxicity data for the solvents are in Supplementary Note 4.

Toxicity data is transformed to the dose required to achieve 50% of the desired response in 50% of the population, ED$_{50}$, during the lifetime. It is assumed that the average bodyweight (bw) is 70 kg, the average inhalation rate (inh) is 13 m^3 day^{-1} and the average lifetime is 70 years. The equation to obtain ED$_{50}$ for oral ingestion and inhalation are, respectively:

$$ED_{o,50} \left(\frac{kg}{person\ lifetime} \right) = D_o \cdot \frac{CD \cdot CF}{AFt_o} \cdot bw \cdot lifetime \cdot 365 \cdot 10^{-6} \tag{1}$$

$$ED_{i,50} \left(\frac{kg}{person\ lifetime} \right) = D_i \cdot \frac{CD \cdot CF}{AFt_i} \cdot inh \cdot lifetime \cdot 365 \cdot 10^{-6} \tag{2}$$

where, AFt$_o$ is the extrapolation factor for interspecies differences (1.1 for pigs, 1.5 for dogs, 1.9 for monkeys or cats, 2.4 for rabbits, 2.6 for hens, 2.9 for minks, 3.1 for guinea pigs, 4.1 for rats, 4.9 for hamsters, 5.5 for gerbils and 7.3 for mice). For inhalation, Aft$_i$ equals 1; CD is a factor to convert subacute and subchronic exposures to chronic exposures (0.5 for subchronic and 0.2 for subacute) and CF is a factor to convert NOAEL/NOAEC and LOAEL/LOAEC to ED$_{50}$ (9 and 2.25, respectively). Results are in Supplementary Table 12.

312   Each one of the identified diseases are associated with one or several codified causes of the Global Burden
313   Disease[60] (GBD 2017). The DALYs per case for each symptom are obtained by dividing global DALYs by the
314   number of incidences in 2017, see Supplementary Table 13.

Solvent removal

316   Common considerations to estimate the energy during the solvent removal process are: initial temperature is 25
317   ºC, T_o, pressure is 1 atm, the volume of air is established to achieve a solvent volume concentration less than
318   30% of the lower explosive limit, (LEL) per industry standards[61,62].

319   Molecular weights and LEL are obtained from PubChem. Heat capacities and vaporization enthalpies are
320   obtained from NIST Chemistry WebBook[63]. Heat capacities of DMI and DMPU are estimated. LEL is the minimum
321   concentration of flammable vapor in air that will propagate a flame if ignited. Experimentally determined values
322   for these parameters are not readily available for many chemicals. LEL was estimated based on the 50% of the
323   stoichiometric concentration of combustion[64].

324   The method by Joback et al. was used to predict the ideal gas heat capacities of solvents without empirical
325   values[65], DMI and DMPU. The estimation of liquid heat capacities are based on ideal gas heat capacities[66,67],
326   calculated as a function of temperature, based on the summation of functional groups present in the molecular
327   structure of the component, and with the estimation of critical properties of the solvents[68]. Heat capacities are
328   in the Supplementary Table 3.

329   Human health impacts due to energy consumption for solvent vaporization are assumed to be electricity for
330   kinetic energy (Electricity, medium voltage, US) and gas for heating (Heat, from steam, in chemical industry,
331   RoW). Energy losses for kinetic energy and heating are estimated for inefficiencies with an extra 30%[69].

332   The solvent can be removed from the perovskite layer through a forced flow of air. This scenario is typically
333   followed in roll-to-roll processes. The transfer mass of the solvent is modelled with equation (3):

$$N_s = k_c \cdot (c_{s1} - c_{s2}) \tag{3}$$

334   where N_s is the molar flux of the solvent and k_c is the mass transfer coefficient expressed, in this case, in units of
335   molar concentration. The concentrations of the solvent in the perovskite and in the air are c_{s1} and c_{s2},
336   respectively. We assume the air is initially free of solvent (c_{s2} is zero). The concentration c_{s1} is obtained from the
337   vapor pressure of the solvent, P_S:

$$c_{s1} = \frac{P_S}{R \cdot T} \tag{4}$$

338   Mass transfer coefficients depend on the relevant physical properties of the air, the geometry and the approach
339   velocity of the air over the perovskite layer. The mass transfer coefficients can be obtained with the
340   dimensionless Sherwood number, Sh:

$$Sh = \frac{k_c \cdot L}{D_{SA}} \tag{5}$$

341   where L is the characteristic length scale and D_{SA} is the diffusion coefficient, in this case, of the solvent in the air.
342   The Sherwood number depends on two dimensionless constants. One is the Reynolds number, Re, and the other
343   is the Schmidt number, Sc:

$$Re = \frac{L \cdot u}{v} \qquad\qquad Sc = \frac{v}{D_{SA}} \qquad\qquad (6)$$

344 Where v and u are the viscosity and the velocity of the air, respectively. The expressions for a flat plate are
345 obtained from the solutions of the boundary layer equations. For a laminar flow, the average Sherwood number
346 is:

$$Sh = 0.664 \cdot Re^{\frac{1}{2}} \cdot Sc^{\frac{1}{3}} \qquad Re < 3 \cdot 10^5 \ \& \ 0.6 \le Sc \le 50 \qquad\qquad (7)$$

347 and for a turbulent flow:

$$Sh = \left(0.037 \cdot Re^{\frac{4}{5}} - 871\right) \cdot Sc^{\frac{1}{3}} \qquad 3 \cdot 10^5 \le Re \le 10^8 \ \& \ 0.6 \le Sc \le 50 \qquad\qquad (8)$$

348 Laminar flow is used in several pre-industrial plants. However, turbulent flow is not sufficiently assessed[44]. In the
349 first approach, the vaporization rate, N_A, is obtained at room temperature (T_o= 25ºC). If the evaporation time of
350 a surface of characteristic length of 1 m and width web of 1 m with 500 nm of thickness is greater than 2
351 seconds, the temperature, T, is increased to 40ºC and above with increments of 10ºC until the evaporation time
352 falls below 2 seconds.

353 Energy consumption is determined by the air kinetic energy, E_c, and the heat for air and for the solvent, Q_A and
354 Q_S, respectively:

$$E = E_c + Q_A + Q_S = \frac{1}{2} \cdot m_A \cdot u^2 + m_A \cdot cp_A \cdot (T - T_o) + m_S \cdot cp_S \cdot (T - T_o) \qquad\qquad (9)$$

355 The air mass, m_A, is established to achieve a solvent volume concentration below 30% of the LEL. The coefficient
356 of diffusion, vapor pressure, viscosity, density and specific heat (cp) are temperature dependent. Air specific
357 heat is obtained for each temperature, however, specific heats for solvents are considered constant. Solvent
358 diffusivities in air are obtained at 25ºC[70,71]. If the value is not experimentally available, it is predicted with a
359 QSPR model[72] for GBL, THF, NMP, DMAC and DMSO. Values are in the Supplementary Table 3. Diffusivities for
360 other temperatures, $D_{AB,T}$, are obtained with the expression[70]:

$$D_{SA,T} = \frac{D_{SA,T}}{\left(\frac{298}{T}\right)^2} \qquad\qquad (10)$$

361 Vapor pressures of the solvents at different temperature are obtained with the Clausius Clapeyron equation:

$$P_T = P_o \cdot e^{\frac{\Delta H_{vap}}{R} \cdot \left(\frac{1}{T_o} - \frac{1}{T}\right)} \qquad\qquad (11)$$

362 Liquid densities of solvents at different temperatures are estimated with the volumetric temperature
363 coefficient, β, obtained for DMF[73].

$$\rho_T = \frac{\rho_o}{1 + \beta \cdot (T - T_o)} \qquad\qquad (12)$$

Condensation of solvent

A condenser connected to the evaporation hood is considered in scenarios 2-4 to avoid the air emission of the solvent. The condensed solvent is either further treated by incineration (scenario 2) or recovered (scenarios 3-4). Condensation is a separation technique in which one or more volatile components of a vapor mixture are separated from the remaining vapors through saturation followed by a phase change. In a condenser, the phase change from gas to liquid is achieved by lowering the temperature at a constant pressure. The US EPA methodology[74] is followed to estimate the energy consumption, assuming a removal efficiency of 90%.

This methodology is complemented with the values of the critical temperatures[75] and the coefficient of performance (COP), as a function of condensation temperature (T_{cd}) of the VOC[45], limited to a maximum value of 3:

$$COP = \min(f(X), 3)$$

$$f(X) = 4 \cdot 10^{-6} \cdot \left(\frac{T_{cd} - 10}{308.15 - T_{cd}}\right)^3 - 0.0025 \cdot \left(\frac{T_{cd} - 10}{308.15 - T_{cd}}\right)^2 + 0.7057 \cdot \left(\frac{T_{cd} - 10}{308.15 - T_{cd}}\right) - 0.4691 \tag{13}$$

Incineration

Hazardous waste incinerations for scenario 2 and for the waste fraction of distillation in scenario 4 are estimated using the model by Doka[76]. Each solvent waste is defined in terms of content of chemical elements (C, H, O, S, N etc.). The environmental benefits of energy recovery (electricity and heat), known as energy credits, are separate from the impacts of incineration. The solid residues generated in incineration are landfilled in a residual material landfill. Life cycle inventories are introduced in SimaPro 9.0[77] and the human health environmental impacts are assessed.

Distillation

Scenario 4 is designed assuming the purity of solvent condensed is not sufficient to be reused directly and distillation is necessary. Average statistical data[78] are taken into account, due to great uncertainty about potential solvent mixtures and impurities in the perovskite layer. Data for electricity and nitrogen are the same for all solvents, 0.12 MJ and 1.88 g respectively, per kg of solvent. The fraction of solvent recovered is 0.71 and the remainder is incinerated accounting for energy recovery.

Thermal energy is the necessary energy to heat the solvent, Q_S, and the nitrogen, $Q_{N,}$ from the initial temperature to the boiling point, T_{bp}, and the heat of vaporization of the solvent, $Q_{S,vap,}$ all multiplied by coefficient of 4 to reach the average statistical data[78]:

$$H = \left(Q_N + Q_S + Q_{s,vap}\right) \cdot coef$$
$$= \left(m_N \cdot cp_N \cdot (T - T_o) + m_S \cdot cp_S \cdot (T - T_o) + m_S \cdot \Delta H_{s,vap}\right) \cdot coef \tag{14}$$

Heat capacities, boiling temperatures and vaporization enthalpies are obtained from NIST Chemistry WebBook[63].

Solvents production

Life cycle inventories for solvent production are obtained from Ecoinvent 3.5[47], with the exception of DMPU and DMI which are obtained from the reactions Scheme 1 and Scheme 2, respectively (listed below).
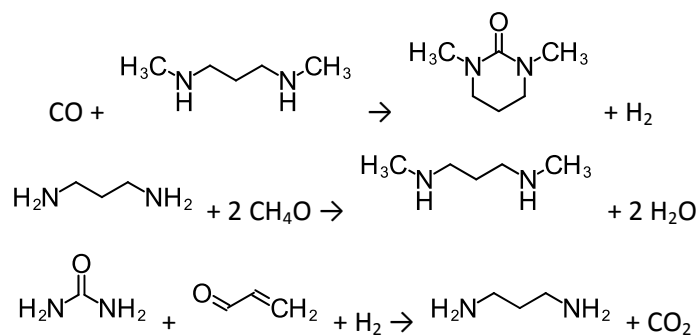
394 *Scheme 1. Synthesis of 1,3-dimethyl-3,4,5,6-tetrahydropyrimidin-2(1H)-one (DMPU).*

395 In the first reaction of Scheme 1, carbon monoxide and N,N'-dimethyl-1,3-propanediamine react to produce 1,3-
396 dimethyl-3,4,5,6-tetrahydropyrimidin-2(1H)-one. Reagents are maintained at 20 ºC for 3 h[79]. In the second
397 reaction, 1,3-diaminopropane and 2 moles of methanol react to produce N,N'-dimethyl-1,3-propanediamine.
398 Reagents are heated to 300 ºC[80]. In the last reaction, urea, acrolein and hydrogen react to produce 1,3-
399 diaminopropane. Reagents are heated to 150 ºC[81].
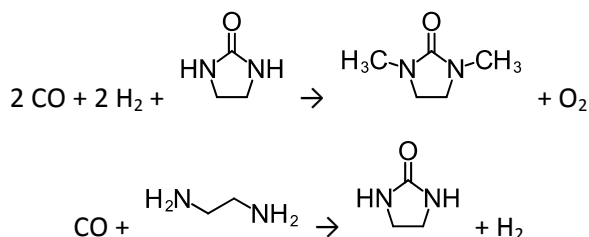
400 *Scheme 2. Synthesis of 1,3-dimethylimidazolidin-2-one (DMI).*

401 Carbon monoxide, hydrogen and imidazolidone react to produce 1,3-dimethylimidazolidin-2-one in the first
402 reaction of Scheme 2. Reagents are heated to 145 ºC for 4 h[82]. In the second reaction, carbon monoxide and
403 ethylenediamine produce imidazolidone and the reagents are maintained at 20 ºC for 4 h[83].

404 In addition to the inputs from the synthesis reactions, average transport for chemicals from a factory is
405 considered[47].

Data Availability

407 The datasets generated during and/or analyzed during the current study are available from the first author on
408 reasonable request.

409

References

1. Kojima, A., Teshima, K., Shirai, Y. & Miyasaka, T. Organometal halide perovskites as visible-light sensitizers for photovoltaic cells. *J. Am. Chem. Soc.* **131**, 6050–6051 (2009).

2. Lee, M. M., Teuscher, J., Miyasaka, T., Murakami, T. N. & Snaith, H. J. Efficient hybrid solar cells based on meso-superstructured organometal halide perovskites. *Science* **338**, 643–7 (2012).

3. Kim, H.-S. *et al.* Lead iodide perovskite sensitized all-slid-state submicron thin film mesoscopic solar cell with efficiency exceeding 9%. *Sci. Rep.* **2**, 591 (2012).

4. NREL. Best Research-Cell Efficiency Chart. *Photovoltaic Research* (2020). Available at: https://www.nrel.gov/pv/cell-efficiency.html. (Accessed: 15th March 2020)

5. Berry, J. J. *et al.* Perovskite photovoltaics: The path to a printable terawatt-scale technology. *ACS Energy Lett.* **2**, 2540–2544 (2017).

6. Quan, L. N. *et al.* Perovskites for Next-generation optical sources. *Chemical Reviews* **119**, 7444–7477 (2019).

7. Jean, J., Woodhouse, M. & Bulović, V. Accelerating photovoltaic market entry with module replacement. *Joule* **3**, 2824–2841 (2019).

8. Ono, L. K., Park, N.-G., Zhu, K., Huang, W. & Qi, Y. Perovskite solar cells—towards commercialization. *ACS Energy Lett.* **2**, 1749–1751 (2017).

9. Galagan, Y. Perovskite solar cells: Toward industrial-scale methods. *Journal of Physical Chemistry Letters* **9**, 4326–4335 (2018).

10. Li, Z. *et al.* Acid additives enhancing the conductivity of spiro-OMeTAD toward high-efficiency and hysteresis-less planar perovskite solar cells. *Adv. Energy Mater.* **7**, 1601451 (2017).

11. Swartwout, R., Hoerantner, M. T. & Bulović, V. Scalable deposition methods for large-area production of perovskite thin films. *ENERGY Environ. Mater.* **2**, 119–145 (2019).

12. European Chemicals Agency. Homepage - ECHA. Available at: https://echa.europa.eu/. (Accessed: 26th September 2019)

13. Jimenez-Gonzalez, C. Life cycle considerations of solvents. *Current Opinion in Green and Sustainable Chemistry* **18**, 66–71 (2019).

14. Celik, I., Song, Z., Phillips, A. B., Heben, M. J. & Apul, D. Life cycle analysis of metals in emerging photovoltaic (PV) technologies: A modeling approach to estimate use phase leaching. *J. Clean. Prod.* **186**, 632–639 (2018).

15. Zhang, J., Gao, X., Deng, Y., Zha, Y. & Yuan, C. Comparison of life cycle environmental impacts of different perovskite solar cell systems. *Sol. Energy Mater. Sol. Cells* **166**, 9–17 (2017).

16. Alberola-Borràs, J.-A. *et al.* Relative impacts of methylammonium lead triiodide perovskite solar cells based on life cycle assessment. *Sol. Energy Mater. Sol. Cells* **179**, 169–177 (2018).

17. Gong, J., Darling, S. B. & You, F. Perovskite photovoltaics: life-cycle assessment of energy and environmental impacts. *Energy Environ. Sci.* **8**, 1953–1968 (2015).

18. Monteiro Lunardi, M., Wing Yi Ho-Baillie, A., Alvarez-Gaitan, J. P., Moore, S. & Corkish, R. A life cycle assessment of perovskite/silicon tandem solar cells. *Prog. Photovoltaics Res. Appl.* **25**, 679–695 (2017).

19. Espinosa, N., Serrano-Luján, L., Urbina, A. & Krebs, F. C. Solution and vapour deposited lead perovskite

14

449 solar cells: Ecotoxicity from a life cycle assessment perspective. *Sol. Energy Mater. Sol. Cells* **137**, 303–310
450 (2015).

451 20. Sánchez, S. *et al.* Flash infrared annealing as a cost-effective and low environmental impact processing
452 method for planar perovskite solar cells. *Mater. Today* **31**, 39–46 (2019).

453 21. Alberola-Borràs, J.-A., Vidal, R. & Mora-Seró, I. Evaluation of multiple cation/anion perovskite solar cells
454 through life cycle assessment. *Sustain. Energy Fuels* **2**, 1600–1609 (2018).

455 22. Alberola-Borràs, J.-A. *et al.* Perovskite photovoltaic modules: Life cycle assessment of pre-industrial
456 production process. *iScience* **9**, 542–551 (2018).

457 23. Gardner, K. L. *et al.* Nonhazardous solvent systems for processing perovskite photovoltaics. *Adv. Energy*
458 *Mater.* **6**, 1600386 (2016).

459 24. Galagan, Y. *et al.* Roll-to-Roll slot die coated perovskite for efficient flexible solar cells. *Adv. Energy Mater.*
460 **8**, 1801935 (2018).

461 25. Wang, J. *et al.* Highly efficient perovskite solar cells using non-toxic industry compatible solvent system.
462 *Sol. RRL* **1**, 1700091 (2017).

463 26. Liu, X., Wu, J., Yang, Y., Wu, T. & Guo, Q. Pyridine solvent engineering for high quality anion-cation-mixed
464 hybrid and high performance of perovskite solar cells. *J. Power Sources* **399**, 144–150 (2018).

465 27. Babaei, A. *et al.* Hansen theory applied to the identification of nonhazardous solvents for hybrid
466 perovskite thin-films processing. *Polyhedron* **147**, 9–14 (2018).

467 28. Noel, N. K. *et al.* A low viscosity, low boiling point, clean solvent system for the rapid crystallisation of
468 highly specular perovskite films. *Energy Environ. Sci.* **10**, 145–152 (2017).

469 29. Zhi, L. *et al.* Perovskite solar cells fabricated by using an environmental friendly aprotic polar additive of
470 1,3-dimethyl-2-imidazolidinone. *Nanoscale Res. Lett.* **12**, (2017).

471 30. Hauschild, M. Z. *et al.* Identifying best existing practice for characterization modeling in life cycle impact
472 assessment. *Int. J. Life Cycle Assess.* **18**, 683–697 (2013).

473 31. Rosenbaum, R. K. *et al.* USEtox human exposure and toxicity factors for comparative assessment of toxic
474 emissions in life cycle analysis: Sensitivity to key chemical properties. *Int. J. Life Cycle Assess.* **16**, 710–727
475 (2011).

476 32. Saouter, E., Biganzoli, F., Pant, R., Sala, S. & Versteeg, D. Using REACH for the EU environmental footprint:
477 Building a usable ecotoxicity database, part I. *Integr. Environ. Assess. Manag.* **15**, 783–795 (2019).

478 33. Capello, C., Fischer, U. & Hungerbühler, K. What is a green solvent? A comprehensive framework for the
479 environmental assessment of solvents. *Green Chem.* **9**, 927–934 (2007).

480 34. Hamill, J. C., Schwartz, J. & Loo, Y. L. Influence of solvent coordination on hybrid organic-inorganic
481 perovskite formation. *ACS Energy Lett.* **3**, 92–97 (2018).

482 35. Gutmann, V. Empirical parameters for donor and acceptor properties of solvents. *Electrochim. Acta* **21**,
483 661–670 (1976).

484 36. Bruening, K. & Tassone, C. J. Antisolvent processing of lead halide perovskite thin films studied by: In situ
485 X-ray diffraction. *J. Mater. Chem. A* **6**, 18865–18870 (2018).

486 37. Cao, X. *et al.* A review of the role of solvents in formation of high-quality solution-processed perovskite
487 films. *ACS Applied Materials and Interfaces* **11**, 7639–7654 (2019).

488   38.   Jung, K., Chae, W.-S., Park, Y. C., Kim, J. & Lee, M.-J. Influence of Lewis base HMPA on the properties of
489   efficient planar MAPbI3 solar cells fabricated by one-step process assisted by Lewis acid-base adduct
490   approach. *Chem. Eng. J.* **380**, 122436 (2020).

491   39.   Guo, L., Wang, O., Zhao, D., Gan, X. & Liu, H. The deposition of (CH3NH3)2Pb(SCN)2I2 thin films and their
492   application in perovskites solar cells. *Polyhedron* **145**, 16–21 (2018).

493   40.   Wang, B., Wong, K. Y., Yang, S. & Chen, T. Crystallinity and defect state engineering in organo-lead halide
494   perovskite for high-efficiency solar cells. *J. Mater. Chem. A* **4**, 3806–3812 (2016).

495   41.   Park, B. W. *et al.* Chemical engineering of methylammonium lead iodide/bromide perovskites: Tuning of
496   opto-electronic properties and photovoltaic performance. *J. Mater. Chem. A* **3**, 21760–21771 (2015).

497   42.   Xie, L., Cho, A.-N., Park, N.-G. & Kim, K. Efficient and reproducible CH3NH3PbI3 perovskite layer prepared
498   using a binary solvent containing a cyclic urea additive. *ACS Appl. Mater. Interfaces* **10**, 9390–9397
499   (2018).

500   43.   Lee, J. W. *et al.* Tuning molecular interactions for highly reproducible and efficient formamidinium
501   perovskite solar cells via adduct approach. *J. Am. Chem. Soc.* **140**, 6317–6324 (2018).

502   44.   Gao, L. L., Zhang, K. J., Chen, N. & Yang, G. J. Boundary layer tuning induced fast and high performance
503   perovskite film precipitation by facile one-step solution engineering. *J. Mater. Chem. A* **5**, 18120–18127
504   (2017).

505   45.   Belaissaoui, B., Le Moullec, Y. & Favre, E. Energy efficiency of a hybrid membrane/condensation process
506   for VOC (Volatile Organic Compounds) recovery from air: A generic approach. *Energy* **95**, 291–302 (2016).

507   46.   Wu, J. J., Muruganandham, M. & Chen, S. H. Degradation of DMSO by ozone-based advanced oxidation
508   processes. *J. Hazard. Mater.* **149**, 218–225 (2007).

509   47.   Ecoinvent. Ecoinvent. (2018). Available at: https://www.ecoinvent.org/references/references.html.
510   (Accessed: 27th September 2019)

511   48.   Masi, S. *et al.* Chemi-Structural Stabilization of Formamidinium Lead Iodide Perovskite by Using
512   Embedded Quantum Dots. *ACS Energy Lett.* 418–427 (2020). doi:10.1021/acsenergylett.9b02450

513   49.   Bruening, K. *et al.* Scalable Fabrication of Perovskite Solar Cells to Meet Climate Targets. *Joule* **2**, 2464–
514   2476 (2018).

515   50.   Rosenbaum, R. *et al.* USEtox—the UNEP-SETAC toxicity model: recommended characterisation factors for
516   human toxicity and freshwater ecotoxicity in life cycle impact assessment. *Int. J. Life Cycle Assess.* **13**,
517   532–546 (2008).

518   51.   Fantke, P. *et al. UNEP/SETAC scientific consensus model for characterizing human toxicological and
519   ecotoxicological impacts of chemical emissions in life cycle assessment. USEtox 2.0 MANUAL: ORGANIC
520   SUBSTANCES (Version 2)*. (2015).

521   52.   Huijbregts, M. A. J. *et al.* ReCiPe2016: a harmonised life cycle impact assessment method at midpoint and
522   endpoint level. *Int. J. Life Cycle Assess.* **22**, 138–147 (2017).

523   53.   OECD. *OECD QSAR Toolbox v.4.3.1*. (2019).

524   54.   US EPA. *Estimation Programs Interface Suite[TM] for Microsoft® Windows, v 4.11*. (2017).

525   55.   Card, M. L. *et al.* History of EPI Suite[TM] and future perspectives on chemical property estimation in US
526   Toxic Substances Control Act new chemical risk assessments. *Environ. Sci. Process. Impacts* **19**, 203–212
527   (2017).

528 56. Müller, N., de Zwart, D., Hauschild, M., Kijko, G. & Fantke, P. Exploring REACH as a potential data source
529   for characterizing ecotoxicity in life cycle assessment. *Environ. Toxicol. Chem.* **36**, 492–500 (2017).

530 57. Igos, E. *et al.* Development of USEtox characterisation factors for dishwasher detergents using data made
531   available under REACH. *Chemosphere* **100**, 160–166 (2014).

532 58. Aurisano, N., Albizzati, P. F., Hauschild, M. & Fantke, P. Extrapolation factors for characterizing freshwater
533   ecotoxicity effects. *Environ. Toxicol. Chem.* etc.4564 (2019). doi:10.1002/etc.4564

534 59. Gustavsson, M. B., Hellohf, A. & Backhaus, T. Evaluating the environmental hazard of industrial chemicals
535   from data collected during the REACH registration process. *Sci. Total Environ.* **586**, 658–665 (2017).

536 60. Institute for Health Metrics and Evaluation, (IHME). Global Burden of Disease Study 2017 (GBD 2017)
537   Data Resources | GHDx. *Institute for Health Metrics and Evaluation, (IHME)* (2019). Available at:
538   http://ghdx.healthdata.org/gbd-2017. (Accessed: 11th November 2019)

539 61. Pask, F. *et al.* Systematic approach to industrial oven optimisation for energy saving. *Appl. Therm. Eng.*
540   **71**, 72–77 (2014).

541 62. Nikolaychik, L. V & Technology, T. N. N. Modeling the drying process of thin coatings. in *IS&T's 50th
542   Annual Conference* 502–507 (1998).

543 63. Linstrom, P. J. & Mallard, W. G. NIST Chemistry WebBook, NIST Standard Reference Database. *NIST
544   Chemistry WebBook* (2017). doi:10.18434/T4D303

545 64. Gooding, C. H. Flash Point and Lower Explosive Limit Estimation. in *Encyclopedia of Chemical Processing
546   and Design: Volume 22 Fire Extinguishing Chemicals to Fluid Flow, Slurry Systems and Pipelines* (ed.
547   Mcketta, J. J.) (Marcel Dekker, 1985).

548 65. Joback, K. G. & Reid, R. C. Estimation of pure-component properties from group-contributions. *Chem.
549   Eng. Commun.* **57**, 233–243 (1987).

550 66. Poling, B. E., Prausnitz, J. M. & O'Connell, J. . *The Properties of Gases and Liquids*. (McGraw-Hill, 2001).
551   doi:10.1021/ja0048634

552 67. Ge, R., Hardacre, C., Jacquemin, J., Nancarrow, P. & Rooney, D. W. Heat Capacities of Ionic Liquids as a
553   Function of Temperature at 0.1 MPa. Measurement and Prediction. *J. Chem. Eng. Data* **53**, 2148–2153
554   (2008).

555 68. Valderrama, J. O. & Robles, P. A. Critical properties, normal boiling temperatures, and acentric factors of
556   fifty ionic liquids. *Ind. Eng. Chem. Res.* **46**, 1338–1344 (2007).

557 69. Avci, A. & Can, M. Analysis of the drying process on unsteady forced convection in thin films of ink. *Appl.
558   Therm. Eng.* **19**, 641–657 (1999).

559 70. Lugg, G. A. Diffusion coefficients of some organic and other vapors in air. *Anal. Chem.* **40**, 1072–1077
560   (1968).

561 71. Tang, M. J., Shiraiwa, M., Pöschl, U., Cox, R. A. & Kalberer, M. Compilation and evaluation of gas phase
562   diffusion coefficients of reactive trace gases in the atmosphere: Volume 2. Diffusivities of organic
563   compounds, pressure-normalised mean free paths, and average Knudsen numbers for gas uptake
564   calculations. *Atmos. Chem. Phys.* **15**, 5585–5598 (2015).

565 72. Mirkhani, S. A., Gharagheizi, F. & Sattari, M. A QSPR model for prediction of diffusion coefficient of non-
566   electrolyte organic compounds in air at ambient condition. *Chemosphere* **86**, 959–966 (2012).

567 73. Zúñiga-Moreno, A. & Galicia-Luna, L. A. Compressed liquid densities and excess volumes for the binary

568 system CO2 + N,N-dimethylformamide (DMF) from (313 to 363) K and pressures up to 25 MPa. *J. Chem.*
569 *Eng. Data* **50**, 1224–1233 (2005).

570 74. Schaffner, K., Bradley, K., Randall, D. & Sorrels, J. L. Chapter 2 - Refrigerated Condensers. in (U.S. EPA,
571   2017).

572 75. Kroenlein, K. *et al.* NIST/TRC Web Thermo Tables (WTT): Critically Evaluated Thermophysical Property
573   Data. (2012). Available at: https://wtt-pro.nist.gov/wtt-pro/#default/B;50,50/A;0,0,508,422;help,about/.
574   (Accessed: 26th November 2019)

575 76. Doka, G. *Life Cycle Inventories of Waste Treatment Services. ecoinvent report n° 13. Part III Lanfills -*
576   *Underground Deposits - Landfarming*. (2003).

577 77. PRé Consultants. SimaPro | The World's Leading LCA Software. *2019* (2019). Available at:
578   https://simapro.com/. (Accessed: 27th September 2019)

579 78. Capello, C., Hellweg, S., Badertscher, B. & Hungerbühler, K. Life-cycle inventory of waste solvent
580   distillation: statistical analysis of empirical data. *Environ. Sci. Technol.* **39**, 5885–5892 (2005).

581 79. Mizuno, T., Nakai, T. & Mihara, M. Efficient solvent-free synthesis of urea derivatives using selenium-
582   catalyzed carbonylation of amines with carbon monoxide and oxygen. *Synthesis (Stuttg).* **2010**, 4251–
583   4255 (2010).

584 80. Oku, T., Arita, Y., Tsuneki, H. & Ikariya, T. Continuous chemoselective methylation of functionalized
585   amines and diols with supercritical methanol over solid acid and acid–base bifunctional catalysts. *J. Am.*
586   *Chem. Soc.* **126**, 7368–7377 (2004).

587 81. Smith, C. W. Method for producing derivatives of hexahydropyrimidine and converting the same to 1, 3-
588   diamines. 1–5 (1953).

589 82. Song, T. *et al.* Synthesis method of 1,3-dimethyl-2-imidazolone. 1–5 (2018).

590 83. Mizuno, T., Takahashi, J. & Ogawa, A. Synthesis of 2-oxazolidones by sulfur-assisted thiocarboxylation
591   with carbon monoxide and oxidative cyclization with molecular oxygen under mild conditions.
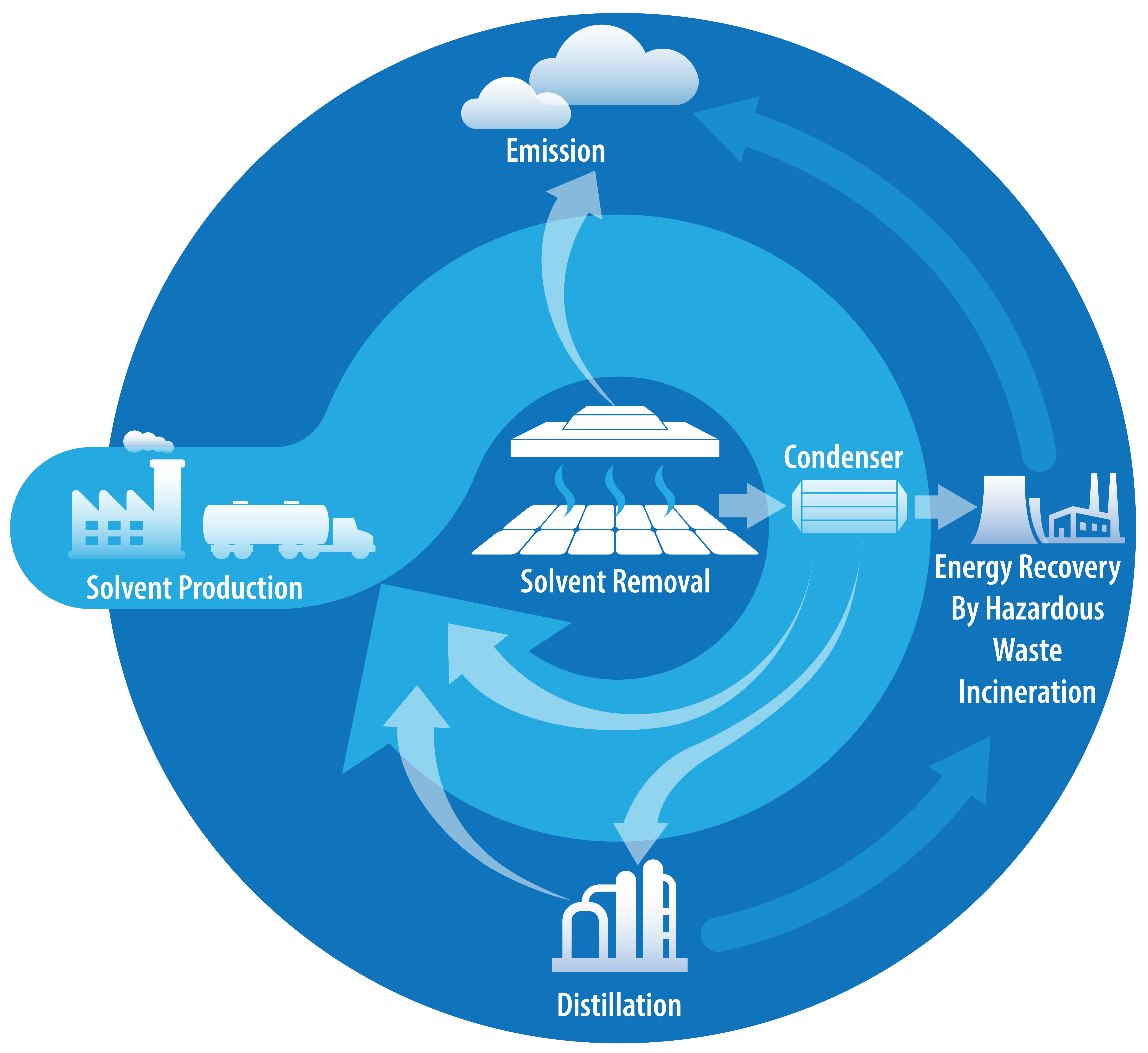592   *Tetrahedron* **58**, 7805–7808 (2002).

593

606

607 **Author contributions.** R.V, J.J.B and J.M.L designed the study. R.V. and J.M.L. wrote the manuscript. R.V.
608 performed the analysis. J.A.A.B modelled DMPU and DMI reaction synthesis. J.L.G.M assembled LCI. D.T.M.

609 reviewed solvent removal. J.M.L, D.T.M and T.H.S. determined solvent selection. I.M.-S. and S.N.H. assisted in
610 the work analysis.

611

612 **Competing financial interests.** The authors declare no competing financial interests.

Emission

Condenser

Solvent Removal

Solvent Production

Energy Recovery By Hazardous Waste Incineration

Distillation

Human Health Toxicity (a) — stacked bar chart showing 10^{-6} DALYs/kg solvent emitted for DMF, DMSO, DMAC, NMP, DMEU, GBL, THF, DMPU with categories: Liver, Fetoxicity, Systemic toxicty, Others.

Human Health Toxicity (b) — grouped bar chart showing 10^{-6} DALYs/kg solvent emitted for DMF, DMSO, DMAC, NMP, DMEU, GBL, THF, DMPU with categories: Initial USETOX, USETOX new data, Modified method.

(a) Human Health Environmental Impacts
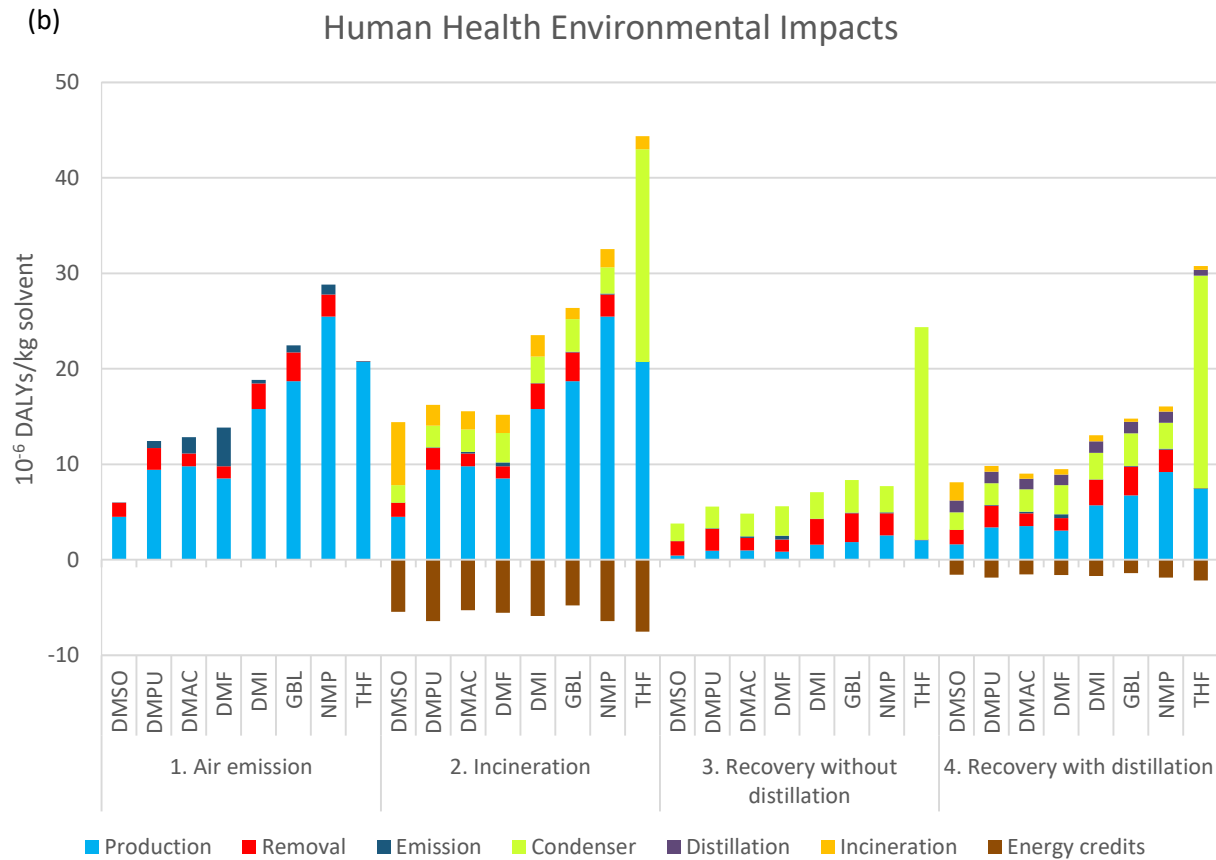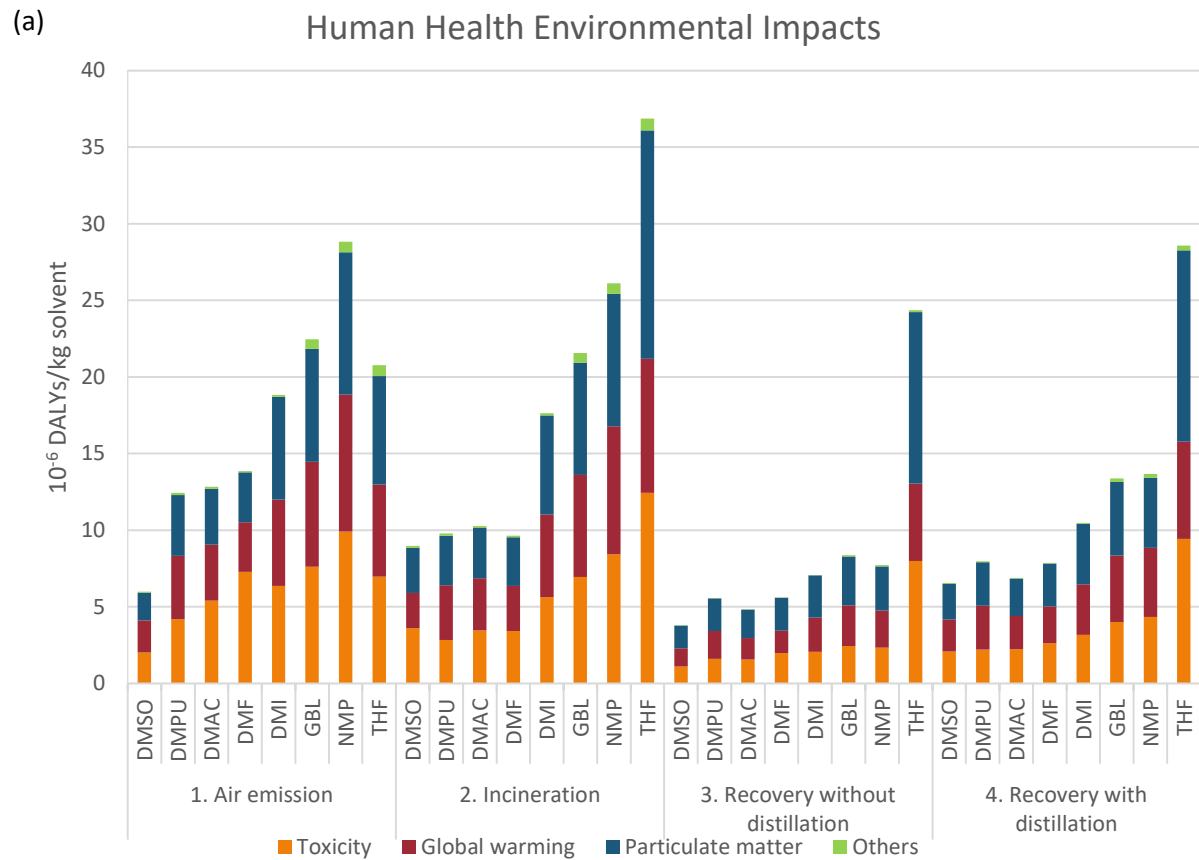
(b) Human Health Environmental Impacts
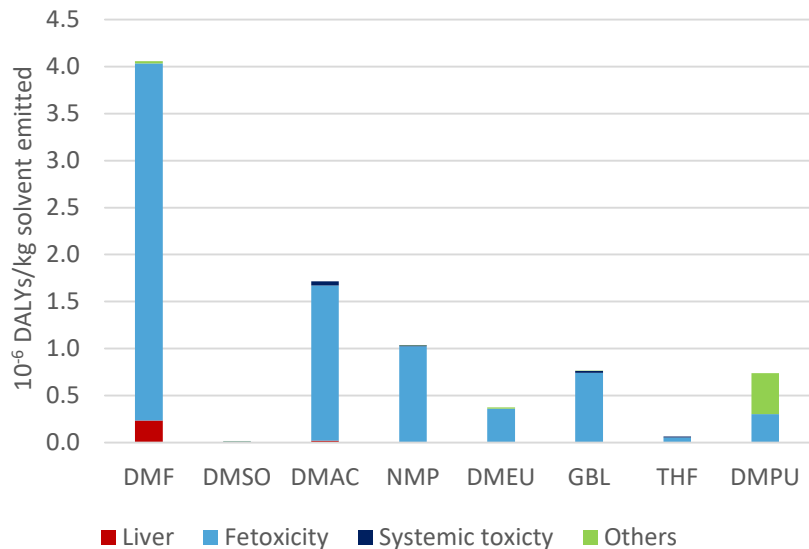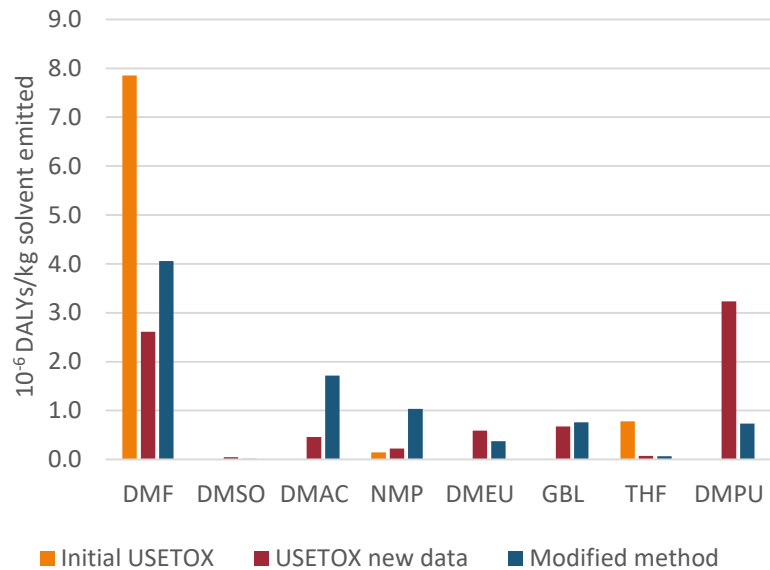
Figure captions:

Figure 1

Figure 1. LCA system boundary schematic showing possible pathways for production of perovskite photovoltaics. The solvents are produced and transported to a factory where perovskites are manufactured. The solvent must then either be emitted to the environment, collected using a condenser for recycling or incineration. If incinerated, additional energy could be recovered. If poised for reuse, additional purification could be required.

Figure 2

*Figure 2. Human health characterization factors expressed in DALYs per kg of substance emitted for the scenario of emission to urban air. **a**, Breakdown by causes with the modified method; **b**, Comparison of the values of USEtox 2.11, the values of USEtox with the new toxicity data and the estimated values with the modified method.*

Figure 3

*Figure 3. Life cycle assessment of 8 aprotic solvents for perovskite film manufacturing with 4 potential scenarios for end-of-life: 1. Air emission of the solvent removed from the thin film; 2. Incineration of condensed solvent with energy production during incineration; 3. Recovery of the condensed solvent without further treatment; 4. Distillation for solvent recovery and unrecovered fraction incinerated. **a**, Breakdown in environmental impact categories; **b**, Breakdown in life cycle phases. Negative values indicate energy credits.*